Electrical Field Effect on CO_2 Absorption and Chemisorption in a Rectangular Bubble Column

Raman Kumar Singh, Prakash Chandra Ghosh, Venkatasailanathan Ramadesigan*

Department of Energy Science and Engineering, IIT Bombay, Mumbai, 400076, India

*Corresponding author email: venkatr@iitb.ac.in

Abstract

The chemisorption and absorption of CO_2 bubbles have been extensively studied and modelled in the literature. CO_2 gas is converted to aqueous CO_2, which produces OH^-, HCO_3^- and CO_3^{2-} ions in the solution. In this study, a three-dimensional multiphase model of a CO_2 bubble column is simulated with and without an electric field using COMSOL Multiphysics. The first model is developed using the Euler-Euler model and simulated using the bubble flow and dilute solution theory module in COMSOL, validated against data obtained from existing literature. The second model builds upon the first model by considering the electrostatic interaction between the charged species and the electrical field, employing the Nernst-Planck equation. Simulation results from the second model indicate that the presence of an electrical field significantly impacts the CO_2 chemisorption process in the rectangular bubble column. The applied field alters the distribution of charged species, influencing concentration gradients and enhancing mass transfer rates. A parametric study is conducted on the applied electric field. The findings of this study can inform on the design of novel CO_2 capture systems, offering potential avenues for mitigating greenhouse gas emissions and advancing sustainable energy practices.

Keywords: Bubble flow, Chemisorption, Dilute solution theory, Computational fluid dynamics, CO_2 Absorption

1 Introduction

In the bubble column, the transfer of mass between gas bubbles and liquid phases is a crucial phenomenon in various fields of chemical engineering, including bioreactors, gas-to-liquid facilities, and the sequestration of carbon dioxide [1]. Currently, there is a focus on studying the chemisorption of CO_2 from flue gas into an aqueous solution of NaOH or KOH due to global warming concerns [2].

Two modelling approaches, the Euler-Euler model (E-E) and the Euler-Lagrange (E-L) model, are the most common and used models for the physisorption and chemisorption of CO_2 in the NaOH or KOH bubble column. The Euler-Euler model uses the volume-averaged and momentum equation to explain the movement over time in both gas and liquid phases. Conversely, the Euler-Lagrange model tracks each bubble using Newton's equation of motion while treating the liquid as a continuum [3].

The gaseous CO_2 is physisorbed and converted into aqueous CO_2, which then reacts with H_2O or OH^- to form aqueous HCO_3^- and CO_3^-. These species are transported through diffusion and convective motion in all regions. The chemisorption reaction in the system is given as:

$$CO_2(aq) + OH^- \longleftrightarrow HCO_3^- \tag{1}$$

$$HCO_3^- + OH^- \longleftrightarrow {CO_3}^{2-} + H_2O \tag{2}$$

The forward and backward reaction rates in the column mainly depend on the forward and backward rate constants and the concentrations of species at that point. Assuming that the forward and backward rate constants for reaction 1 are k_{1f} and k_{1b}, while for the reaction 2 are k_{2f} and k_{2b}, the reaction rate can be written as:

$$R_{1f} = k_{1f} c_{CO_2(aq)} c_{OH^-} \tag{3}$$

$$R_{1b} = k_{1b} c_{HCO_3^-} \tag{4}$$

$$R_{2f} = k_{2f} c_{HCO_3^-} c_{OH^-} \tag{5}$$

$$R_{2b} = k_{2b} c_{{CO_3}^{2-}} \tag{6}$$

The reaction rate is dependent on the local concentration of the species. As reported in the literature, the concentration of gaseous CO_2 is high at the inlet and middle of the column, showing that the aqueous CO_2 concentration conversion rate is high in this region [4].

In the presence of the electric field, the movement of the ionic species is affected. When the electric field is applied to the system positively charged ionic molecule is attracted towards the negative pole while a negatively charged ionic molecule is towards the positive pole. In the CO_2 bubble column, four charged species Na^+, OH^-, HCO_3^- and CO_3^- are present. In the presence of an electric field, the movement of these species will be affected by the migration, hence the local concentration of the species. Due to this production/consumption rate of all species will be affected.

This study combines dilute solution theory with the migration of ions in the electric field, using an E-E model to examine the impact of several important factors. These include mass transfer, local concentration distribution, aqueous convective motion, and bubble flow pattern in the bubble column. The model's development is outlined in the following section. The simulation results are then discussed, followed by conclusions.

2 Model development

2.1 Mass transfer of CO_2 from the gas phase to the liquid phase

A simplified Euler-Euler model is used with this assumption that both gas phases share the same pressure file and the gas density is much less compared to the liquid density. Hence, it is negligible for the momentum equation. Hence, the momentum equation can be written as [5]:

$$\alpha_l \rho_l \frac{\partial u_l}{\partial t} + \alpha_l \rho_l (u_l \cdot \nabla) u_l = \nabla \cdot \left[p + \alpha_l \mu_l (\nabla u_l + (\nabla u_l)^T - \frac{2}{3} (\nabla \cdot u_l) I) \right] + \alpha_l \rho_l g + F \tag{7}$$

The continuity equation can be written as:

$$\frac{\partial}{\partial t} (\rho_l \alpha_l + \rho_g \alpha_g) + \nabla \cdot (\rho_l \alpha_l u_l + \rho_g \alpha_g u_g) = 0 \tag{8}$$

Where α_l, ρ_l, u_l, α_g, ρ_g, and u_g are liquid volume fraction, liquid phase density, liquid phase velocity vector, phase volume fraction, gas phase density, and gas phase velocity vector respectively. g represents gravity and p represents pressure. F is interface forces, a combination of the drag, lift, and virtual mass forces as:

$$F = F_{L,D} + F_{L,L} + F_{L,VM} \tag{9}$$

These forces can be defined as [6]:

$$F_{L,D} = \frac{3}{4} \alpha_g \rho_l \frac{C_D}{d_b} |u_g - u_l| (u_g - u_l) \tag{10}$$

$$F_{L,L} = \alpha_g \rho_l C_L (u_g - u_l) \times \nabla \times u_l \tag{11}$$

$$F_{L,VM} = \alpha_g \rho_l C_{VM} (\frac{d}{dt} u_g - \frac{d}{dt} u_l) \tag{12}$$

Where d_b, C_D, C_L, and C_{VM} are the gas bubble diameter, drag coefficient, lift force constant, and virtual mass coefficient, respectively.

The continuity equation for effective density when mass transfers from gas to liquid happen can be defined as [7]:

$$\frac{\partial (\alpha_g \rho_g)}{\partial t} + \nabla \cdot (\alpha_g \rho_g u_g) = -m_{gl} \tag{13}$$

Where m_{gl} is the interface mass transfer rate for the CO_2 gas and defined according to two film theory as:

$$m_{gl} = k_l a E \rho_l (c_l - c_{CO_2}) M_{CO_2} \tag{14}$$

Where k_l and E are the mass transfer coefficient and enhancement factor. $a = 6\alpha_g / d_b$ is the interfacial area. c_{CO_2} is CO_2 concentration in the liquid phase, and c_l is the dissolved gas in the liquid phase, can be determined by Henry's law as:

$$c_l = \frac{p + p_{ref}}{H_{CO_2}} \tag{15}$$

H_{CO_2} is Henry constant; this is calculated according to Weisenberger and Schumpe method as [8]:

$$\log \frac{H^w_{CO_2}}{H_{CO_2}} = \sum (h_i + h_g)c_i \tag{16}$$

Where h_i and h_g are constant and h_g is linear function of temperature as:

$$h_g = h_{g,o} + h_T(T - 298.15K) \tag{17}$$

$H^w_{CO_2}$ is Henry constant of CO_2 in pure water and can be calculated as:

$$H^w_{CO_2} = 3.59 \times 10^{-7} RT \exp \frac{2044}{T} \tag{18}$$

The mass transfer coefficient is related to the Reynolds number ($Re = \rho_l |u_l - u_g| d_b \mu_l^{-1}$) and Schmidt number ($Sc = \mu_l (\rho_l D_{CO_2})^{-1}$) as [2]:

$$k_l = \frac{D_{CO_2}}{d_b}(2 + 0.015 Re^{0.89} Sc^{0.79}) \tag{19}$$

2.2 Mass balance and mass transport in aqueous electrolyte

A total of four ionic species Na^+, OH^-, HCO_3^-, CO_3^{2-} and one non-ionic species aqueous CO_2 are present in the electrolyte solution. Since the concentration of these species is much less than aqueous electrolyte, these species are treated as dilute solutions. The mass conservation equation as per the dilute solution theory can be written as:

$$\frac{\partial(\alpha_l c_i)}{\partial t} = -\nabla \cdot N_i + \alpha_l S_i \tag{20}$$

c_i represents the concentration of species i. The concentration flux $\overrightarrow{N_i}$ can be written as:

$$N_i = -D_i^{eff} \nabla c_i - z_i \frac{D_i^{eff}}{RT} F \nabla \phi_l + u_l c_i \tag{21}$$

S_i is the production or consumption of species i, can be defined as:

$$S_{CO_{2(aq)}} = \frac{m_{gl}}{M_{CO_2}} - R_{1f} + R_{1b} \tag{22}$$

$$S_{CO_3^{2-}} = R_{2f} - R_{2b} \tag{23}$$

$$S_{HCO_3^-} = R_{1f} - R_{1b} - R_{2f} + R_{2b} \tag{24}$$

$$S_{OH^-} = -R_{1f} + R_{1b} - R_{2f} + R_{2b} \tag{25}$$

D_i^{eff} is the effective diffusion coefficient and calculated according to the Brugmemann correlation as:

$$D_i^{eff} = \alpha_l^{1.5} D_i \tag{26}$$

z_i, R, T, F, and ϕ_l represent the charge number, gas constant (8.314 $\mathrm{J\,mol^{-1}\,K^{-1}}$), operating temperature, Faraday constant (96485 $\mathrm{C\,mol^{-1}}$), and electrolyte potential, respectively. $\nabla\phi_l$ only works for ionic species, yielding zero for non-ionic species.

The solution is electrochemically neutral and mathematically represented as:

$$\sum z_i c_i = 0 \tag{27}$$

2.3 Initial and boundary condition

Initially, it is assumed that the pH of the column is 12, resulting in the concentration of Na^+ and OH^- being 0.01 M and the other species concentration is zero. The pressure in the column is corrected due to gravity by $-\rho_l g(z-h)$. The schematic representation of the bubble column is shown in fig. 1a. Assuming the center of the bottom inlet as 0.03 x 0.03 $\mathrm{m^2}$, the gas velocity is 0.1125 $\mathrm{m\,s^{-1}}$ and the slip velocity is 0.20 $\mathrm{m\,s^{-1}}$. The outlet condition is given at the top of the column. Along the y-axis, different electrolyte potential is applied.

Table 1: *Parameters used in model [6, 9]*

Parameter	Value Unit	Parameter	Value Unit
C_D	1.071	C_L	0.50
$(C_{VM,h}, C_{VM,v})$	$(0.25, 1.53)$	ρ_l	1000 $\mathrm{kg\,m^{-3}}$
ρ_g	1.29 $\mathrm{kg\,m^{-3}}$	μ_l	0.001 $\mathrm{kg\,m^{-1}\,s^{-1}}$
μ_g	1.812×10^{-5} $\mathrm{kg\,m^{-1}\,s^{-1}}$	d_b	5 mm
$D_{\mathrm{CO_2}}$	1.699×10^{-9} $\mathrm{m^2\,s^{-1}}$	$D_{\mathrm{OH^-}}$	5.3×10^{-9} $\mathrm{m^2\,s^{-1}}$
$D_{\mathrm{HCO_3^-}}$	1.1×10^{-9} $\mathrm{m^2\,s^{-1}}$	$D_{\mathrm{CO_3^{2-}}}$	1.5×10^{-9} $\mathrm{m^2\,s^{-1}}$
$D_{\mathrm{Na^+}}$	1.699×10^{-9} $\mathrm{m^2\,s^{-1}}$	k_{2f}	1×10^{5} $\mathrm{m^3\,mol^{-1}\,s^{-1}}$
k_{2b}	2.15×10^{-4} $\mathrm{s^{-1}}$		

2.4 Simulation Setup

COMSOL Multiphysics 6.1 is used to simulate the transient model represented by equations (7) to (27). The model utilizes modules for bubbly flow and laminar flow to convert gaseous CO_2 to aqueous CO_2. Other modules include tertiary electroneutrality for transporting ionic species in the presence of an electric field and transport of dilute species module for the non-ionic species. The relative tolerance is set as 1×10^{-3}.

3 Results and discussion

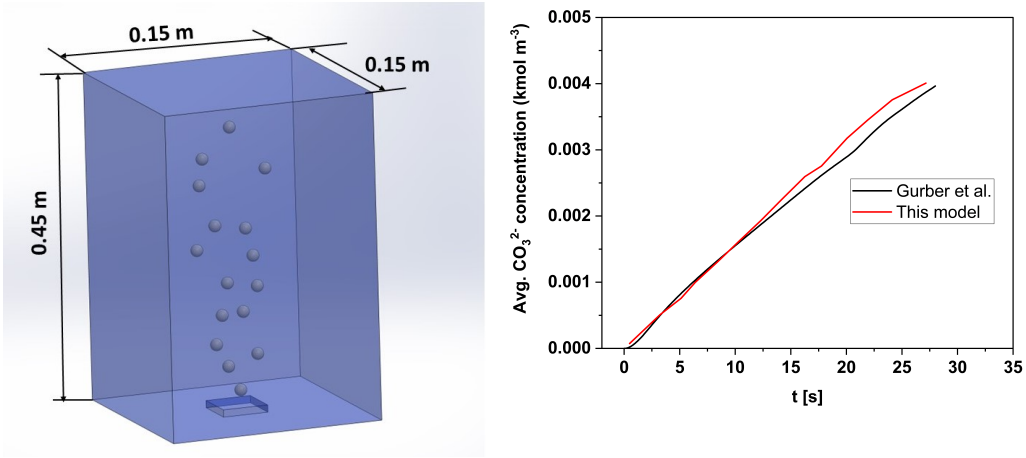

(a) (b)

Figure 1: ***a.*** *Schematic representation of bubble column* ***b.*** *Comparison of simulation data with Gurber et al. results [10]*

3.1 Model validation

The simulations are performed without an electric field for up to 30 seconds and validated with the results obtained by Gruber et al. [10] for the species CO_3^{2-} concentration, which show a good agreement between both models as shown in section 3. Here, the electroneutrality condition is applied, and the concentration of HCO_3^- is calculated. A mesh size with 437 domain elements was used for this study.

3.2 Physisorption of the CO_2 bubble

CO_2 gas is converted into aqueous CO_2 through physisorption. The volume-averaged fraction of the gas phase increases fast initially and is constant for up to 20 seconds. After 20 seconds, the volume fraction is increased as shown in fig. 2a. Interestingly, the average volume fraction of the gas phase does not change with the change in the voltage. This effect happens due to the constant mass transfer rate of 2.1310×10^{-4} $\mathrm{m\,s^{-1}}$ being used at the all applied voltages.

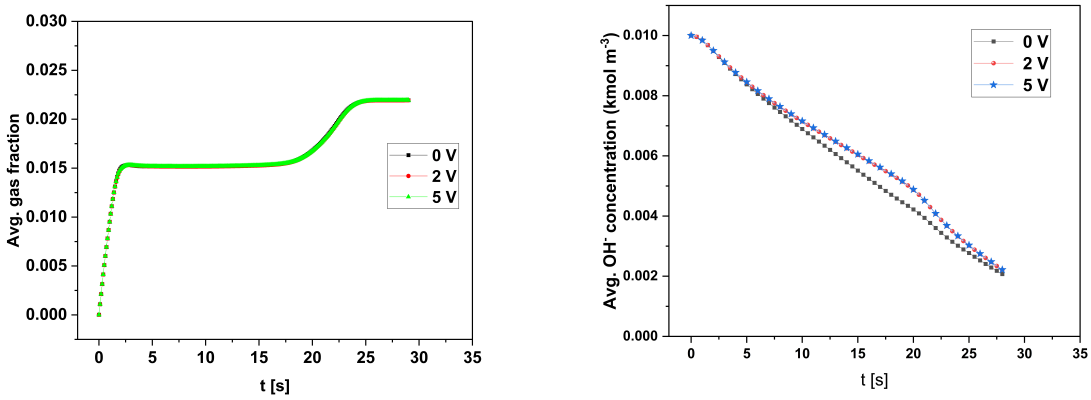

(a) (b)

Figure 2: *Volume-averaged* ***a.*** *Gas phase fraction* ***b.*** *OH^- ion concentration*

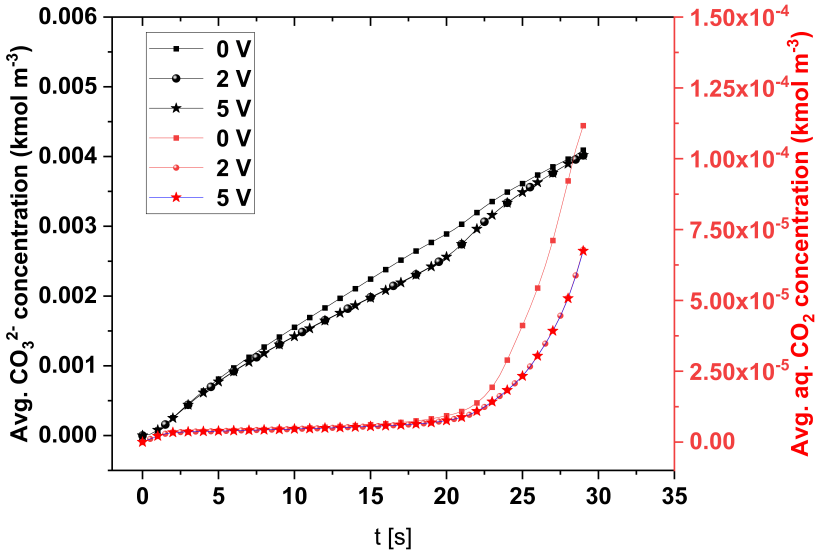

Figure 3: Volume-averaged CO_3^{2-} and CO_2 concentration

3.3 Chemisorption of aqueous CO_2

Aqueous CO_2 reacts with water and produces HCO_3^- and CO_2^{2-} ions in the solution. There are four ionic species Na^+, OH^-, HCO_3^- and CO_3^{2-} whose local concentration will be affected by the presence of an electric field. The volume-averaged concentration of CO_2 and CO_3^- are shown in fig. 3. The concentration of CO_2 gradually increases, but after 20 seconds, it rapidly rises. This shows that the amount of dissolved CO_2 is converted to carbonate and bicarbonate products very fast initially. Similarly, the concentration of CO_3^{2-} can be observed to be increasing with time.

The volume-averaged concentration trends of OH^- are shown in fig. 2b. The OH^- ion concentration is decreasing over time, indicating the consumption of OH^- ion and production of bicarbonate and carbonate ion as mentioned in reaction eq. (1) and eq. (2).

Snapshots of the local concentration distribution of the CO_3^{2-} are shown in fig. 4b at the zy-plane at 0.075 m width. In this study, the voltage is applied to the right side of the column. Figure 4a indicates that the distribution of CO_3^{2-} concentration is randomly distributed and almost similar in all regions, while fig. 4b and fig. 4c show the orientation of negative CO_3^{2-} ions towards the positive side (where electrolyte voltage is applied) of the bubble column. It shows that CO_3^{2-} concentration is high towards

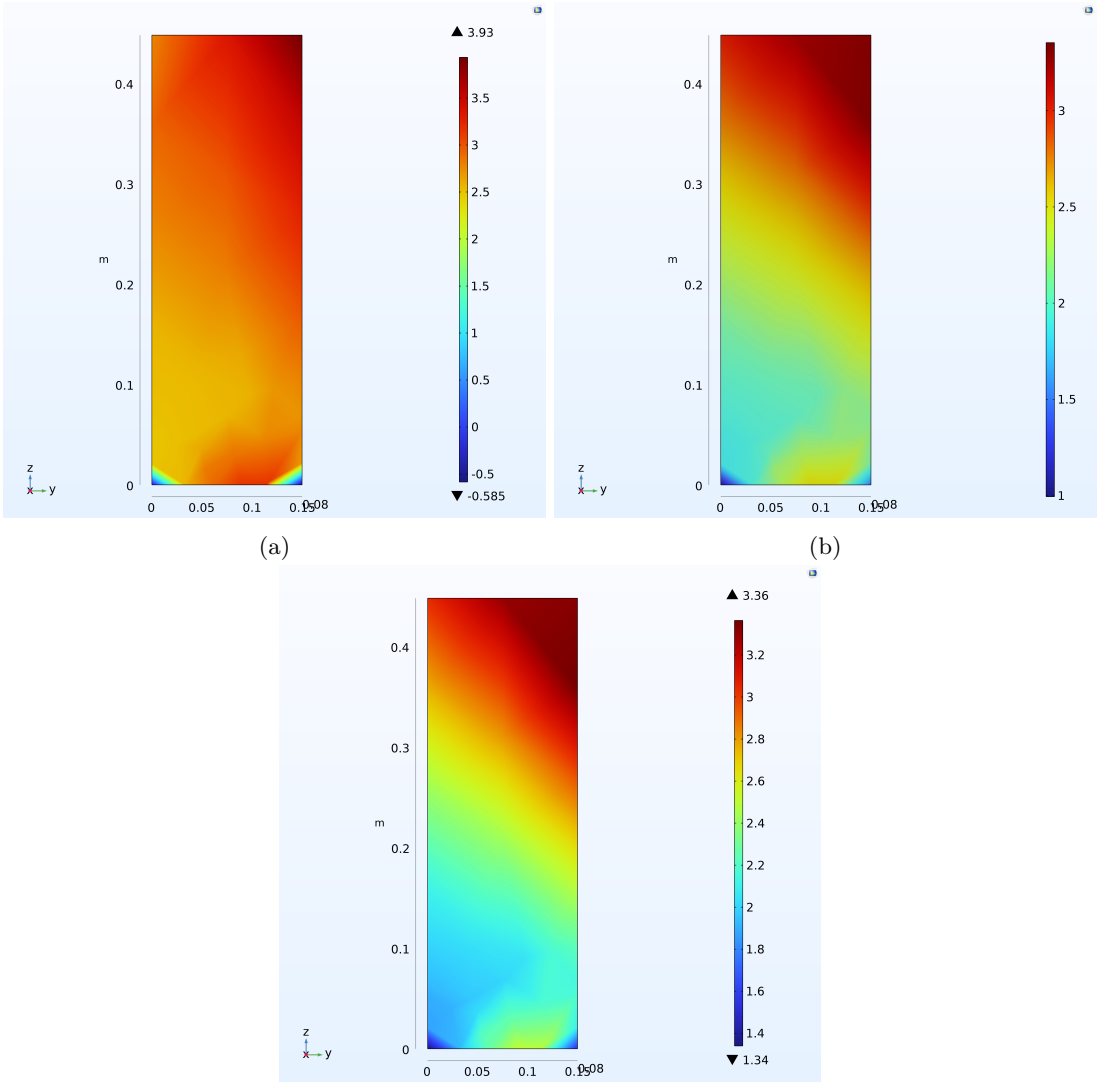

Figure 4: *Snapshot of local concentration distribution of* CO_3^{2-} ion at zy-plane with $x = 0.075$ m after 20 s **a.** At 0 V **b.** At 2 V **c.** At 5 V

the right side and top of the bubble column.

The concentration of CO_2 decreases with the applied potential, indicating that the consumption is faster at this potential as shown in fig. 3. CO_3^{2-} concentration decreases, indicating production of this species is decreasing with the potential. The trends of OH^- ion concentration with potential is shown in fig. 2b.

4 Conclusion

A transient three-dimensional multiphase bubble column is developed using the Euler-Euler model, dilute solution theory with the Nernst-Plank equation in the presence of an electric field. The results obtained from this model are validated from the literature. In the presence of an electric field, it is observed that all the ionic species are oriented towards one side, which affects reaction kinetics, displaying a change in all CO_2, HCO_3^-, OH^- and CO_3^{2-} species concentration trends. Aqueous CO_2 and CO_3^{2-} concentration trends decrease while OH^- concentration trends increase with the applied potential. There are no effects observed in the gas-to-liquid mass transfer rate, gas volume fraction, and concentration trends with different applied voltages of 2 V and 5 V.

The bubble column performance can be increased by adjusting the pH level, applied electric field, gas-to-liquid mass transfer rate, reaction kinetics, and other parameters. This modelling approach can be

used to control the Co_2 conversion reactions in a bubble column with the help of an electric field or in an electrochemical device optimization where CO_2 gases are used in aqueous electrolyte like: $Al-CO_2$, $Zn-CO_2$ or electrochemical CO_2 reduction in aqueous electrolyte.

Acknowledgment

The authors are thankful for the financial support provided by the India–UK Centre for Education and Research in Clean Energy (IUCERCE) (Grant No. DST/RCUK/JVCCE/2015/04(IITB)), funded by the Department of Science and Technology (DST), Government of India.

References

[1]. S Abe, H Okawa, S Hosokawa, and A Tomiyama. Dissolution of a carbon dioxide bubble in a vertical pipe. *Journal of Fluid Science and Technology*, 3(5):667–677, 2008.

[2]. M Krauβ and R Rzehak. Reactive absorption of CO_2 in NaOH: Detailed study of enhancement factor models. *Chemical Engineering Science*, 166:193–209, 2017.

[3]. D Darmana, NG Deen, and JAM Kuipers. Detailed modeling of hydrodynamics, mass transfer and chemical reactions in a bubble column using a discrete bubble model. *Chemical engineering science*, 60(12):3383–3404, 2005.

[4]. J Liu, P Zhou, L Liu, Si Chen, Y Song, and H Yan. Cfd modeling of reactive absorption of CO_2 in aqueous naoh in a rectangular bubble column: Comparison of mass transfer and enhancement factor model. *Chemical Engineering Science*, 230:116218, 2021.

[5]. T. V. William. CFD Module User 's Guide. *CFD Module User's Guide*, pages 1–710, 2017.

[6]. D Zhang, NG Deen, and JAM Kuipers. Numerical modeling of hydrodynamics, mass transfer and chemical reaction in bubble columns. In *6th International Conference on Multiphase Flow, ICMF 2007*, 2007.

[7]. D Zhang, N G Deen, and JAM Kuipers. Euler- euler modeling of flow, mass transfer, and chemical reaction in a bubble column. *Industrial & engineering chemistry research*, 48(1):47–57, 2009.

[8]. S Weisenberger and d A Schumpe. Estimation of gas solubilities in salt solutions at temperatures from 273 k to 363 k. *AIChE Journal*, 42(1):298–300, 1996.

[9]. N Gupta, M Gattrell, and B MacDougall. Calculation for the cathode surface concentrations in the electrochemical reduction of CO_2 in khco3 solutions. *Journal of applied electrochemistry*, 36(2):161–172, 2006.

[10]. M C Gruber, S Radl, and J G Khinast. Rigorous modeling of CO_2 absorption and chemisorption: The influence of bubble coalescence and breakage. *Chemical Engineering Science*, 137:188–204, 2015.